



Development and Characterization of Rice Husk Ash-based Photocatalyst for Degradation of Methylene blue

Olusegun Ayoola Ajayi^{1*}, Oluwafunto Oyinkan Okeniyi^{1**},
Ojo Adefela Adekunle¹, Yahaya Muhammad Sani¹

¹Department of Chemical Engineering, Faculty of Engineering, Ahmadu Bello University, Zaria, 870001, Nigeria

*Corresponding author, Email address: segeaj@gmail.com

**Corresponding author, Email address: funtookeniyi@yahoo.com

Received 30 Oct 2021,
Revised 26 Nov 2021,
Accepted 28 Nov 2021

Keywords

- ✓ ZnO-CuO,
- ✓ Methylene Blue
- ✓ Sol-gel Method,
- ✓ Rice Husk Ash,
- ✓ Photocatalyst.

funtookeniyi@yahoo.com
Phone: +2348068075482;

Abstract

The study utilized agricultural waste, rice husk ash (RHA) for synthesizing ZnO-CuO/RHA catalyst via a modified sol-gel method by Widiarti *et al.*, 2017. The RHA served as a base, and an enhancement for the active photocatalytic sites, i.e., ZnO-CuO. Characterization of the as-synthesized catalysts were conducted with SEM-EDX spectroscopy, FTIR, XRD and BET. The BET results showed an increased surface area of 36.0067 m²/g against the open literature value of 28.74 m²/g. The observed 2θ peaks at 36.75°, 57.39°, 66.42°, and 69.73° for ZnO-CuO/RHA were in concurrence with the crystal planes in the JCPDS 36-1451 cards of ZnO, CuO and SiO. Similarly, the FTIR showed vibrations at 470.65 cm⁻¹, 694.40 cm⁻¹ and 2330.09 cm⁻¹ for ZnO, CuO and RHA (SiO), respectively. The SEM-EDX analysis revealed the morphology of the catalyst as a petal-shaped structure, while that of the RHA was a flaky plate-like structure that facilitated the growth of the active sites. The ZnO-CuO/RHA catalyst was found to possess a higher photocatalytic activity in the presence of sunlight in comparison with ZnO-CuO since using RHA as a base for ZnO-CuO increased the surface area resulting in more active sites under visible light irradiation.

1. Introduction

Global societal and industrial developments are increasing environmental problems with concomitant water pollution getting worrisome. The discharge of wastewater most times includes organic dyes, which are usually hazardous to human health [1]. Water pollution caused by industrial effluents and organic dyes are gaining attention due to their stable and recalcitrant nature to temperature, sunlight and chemicals [2].

The presence of dye effluents has resulted to intractable environmental problems due to the discharge of effluents from the associated processes. These dye effluents can cause damage to living things in water by reducing light penetration and inhibition of photosynthesis leading to damage of internal organs in aquatic beings, and on land it can reduce the soil fertility thereby hindering seed germination and reducing chlorophyll and protein contents in plants [3]. Dye effluents can also result in allergies, skin irritation, cancer, and various health disorders like nausea, vomiting and paralysis [4].

Protecting the environment is one of the important goals of advances in research and development. Hence, reusing wastes and substances that are hitherto of less economic value from various human activities serves as effective means of reducing environmental impact. Rice husk is a residue from rice production that is not scarce but serves as versatile material for various economic purposes [5].

There are various methods currently available for treating dye effluents, namely physical, electrochemical, chemical, and biological methods [6]. However many of them are unable to fully remove the dyes which are then easily transported through sewers and river and may percolate into ground water thereby posing a threat to the quality of the ground water and the socio-economic living of individuals who depend on this water for various purposes [7]. Recently, the process of photocatalytic degradation has served as a method for the removal/destruction of organic pollutants in effluents.

Sunlight irradiation is one of the most readily available sources of clean energy that cannot diminish, hence it is important to carry out research and develop catalysts that can harness irradiation from the sun efficiently and utilize it for management of environmental pollution. Photocatalysis can utilize solar energy as a sustainable technology for the activation of chemical reactions (oxidation and reduction) in providing solutions for water pollution. Although a lot of semiconductors has been used as photocatalysts, many have unsuitable band positions which aids proton reduction, low photo-response and poor stability [8]. The tuning and manipulation of band structures via design and synthesis techniques lead to the improvement of the photocatalytic materials in terms of, reactivity, charge separation, optical/ photo response and stability [9].

In recent years, semiconductors like Stannous oxide (SnO), Zinc oxide (ZnO), Titanium dioxide (TiO₂), Zinc sulfide (ZnS) and Iron(III) oxide (Fe₂O₃) have proven to be effective photocatalysts owing to a higher stability and higher conductivity in comparison to metals and insulators respectively [10]. Metal oxides semiconductor such as TiO₂, Bi₂O₃, Fe₂O₃ are used widely in photocatalysis, sensors, photoemission etc.

Photocatalytic composites are heterogeneous materials made to achieve novel or new properties by tuning properties like band gap, thermal property, magnetic property, optical and mechanical properties [11]. A composite comprising of zinc oxide, copper (II) oxide and rice husk was prepared in this paper due to the properties of each material to achieve a novel composition of SiO-ZnO-CuO without first extracting the SiO from the rice husk ash. Zinc oxide (ZnO) possesses a wide band gap of 3.37 eV and a large exciton binding energy of ~60 meV which has the ability to absorb a wide range of the solar light spectrum at ambient temperature and is a leading catalyst for environmental sustainability as it is stable under chemical, thermal, and high energy radiation conditions with little or no risk to the environment and having a large range for usage [12]. However, a major setback is the large band gap which reduces light absorption capacity in the visible region resulting in fast recombination of photogenerated charges thereby causing a reduction in the photocatalytic efficiency [8].

Copper (II) oxide (CuO), a p-type semiconductor has a band gap of 1.2 eV which can be used for photodegradation of organic compounds due to its photoconductive and photochemical properties [13]. These organic compounds possess metastable phases that needs to be stabilized before photocatalytic application. Rice husk ash (RHA) is a low-cost agro based waste material that serves as a source of silica and is readily available for application in various fields; as an energy source [14]–[16] as an adsorbent for organic molecules and metals from aqueous media [17] well as in the field of effluent treatment as either an adsorbent or as a substrate [18]. Rice husk ash is generated from the burning of rice-husk during which cellulose and lignin are removed to remain silica ash.

Composites can be synthesized by various methods including sol-gel, co-precipitation, wet impregnation, and thermal decomposition [19]. However, sol-gel serves as one of the most preferable methods available due to its stability and versatility of processing. Furthermore, it requires low processing temperature and the resultant particles synthesized are highly homogenized [20].

Accordingly, this work set out to synthesize a novel agro-based photocatalyst using sol-gel method, for there is no known agro-based sunlight driven photocatalysts having rice husk ash (an agricultural waste) as constituent in the open literature. The study therefore investigated the prospects of utilizing low-cost rice husk ash for synthesizing photocatalyst with higher surface area suitable for use in environmental purification via modified sol-gel method. The process promises to be affordable and sustainable.

Novelty aspect: Although a lot of semiconductors has been used as photocatalysts, many have unsuitable surface areas. We have shown that a novel composition of SiO-ZnO-CuO without first extracting the SiO from the rice husk ash confers greater surface area on the photocatalysts. The prospects of this promising modified sol-gel method are intriguing considering its benign and less intensive nature. It also serves as a simpler process in producing photocatalyst with high stability and activity, suitable for use in environmental purification.

2. Methodology

2.1 Sourcing and preparation of Materials

Rice husk ash, Zinc acetate dihydrate $\text{Zn}(\text{CH}_3\text{COO})_2 \cdot 2\text{H}_2\text{O}$ 98% (Merck), copper sulphate pentahydrate $\text{CuSO}_4 \cdot 5\text{H}_2\text{O}$ 98% (Merck), Citric Acid, Ethylene glycol, $\rho = 1.11 \text{ g/mL}$ (Merck) and distilled water were utilized as raw materials. All reagents used were without further purification and of analytical grade.

2.2 Experiments

2.2.1 Preparation of Rice Husk Ash

The rice husk was obtained from a local rice mill in Samaru, Zaria. It was soaked in water and rigorously washed with tap water to remove dirt and dried. The dried cleaned rice husk was ashed by calcining at 700°C in an automated muffle furnace. The rice husk ash (RHA) was soaked and parboiled in 13 mol.dm^{-3} sulphuric acid solution at 175°C for 20 mins under vigorous stirring and then re-washed with distilled water. The resulting slurry was treated with 0.5 mol.dm^{-3} NaOH solution (1:20) and thoroughly washed with deionized water after which it was dried at a room temperature and ground to powder.

2.2.2 Synthesis of ZnO-CuO/RHA

ZnO-CuO/RHA powder was synthesized with sol-gel method as reported by Widiarti *et al.*, 2017 by mixing 5.33 g of zinc (II) acetate dihydrate, 25 ml ethylene glycol, 25 ml distilled water, and 6.3 g citric acid with a magnetic stirrer (SearchTech Instruments, 78HW-1) for 1 hour. Subsequently, 1.27 g copper (II) sulfate pentahydrate with varying weights (1-5 g) rice husk ash (RHA) were added and stirred vigorously at 60°C for 3 hours. The RHA added to the present study served as the modification from that of Widiarti *et al.*, 2017. The slurry was aged for 36 hours in dark cupboard, until the gel turned into a greenish colloidal suspension. The gel was washed with distilled water, dried and ground to a powdery form before calcination at 550°C for 4 h in a muffled furnace (Model 5300A30/F6010-TS) to obtain ZnO-CuO/RHA powder. [Figure 1](#) presents the schematic flow diagram for synthesizing ZnO-CuO/RHA.

2.2.3 General procedure for the photocatalytic degradation

The photocatalytic activity of ZnO-CuO/RHA for the degradation of methylene blue was conducted under sunlight irradiation at ambient temperature. The experiment was conducted in a

beaker with continuous magnetic stirring at 500 rpm for varying reaction time. The reactants (methylene blue and ZnO-CuO/RHA catalyst) were stirred in darkness for 30 minutes to establish equilibrium for adsorption-desorption between the surface of the photocatalyst and the dye under ambient conditions after which it was exposed to sunlight irradiation with intensity of 78560 W/m² to aid the photocatalytic degradation.

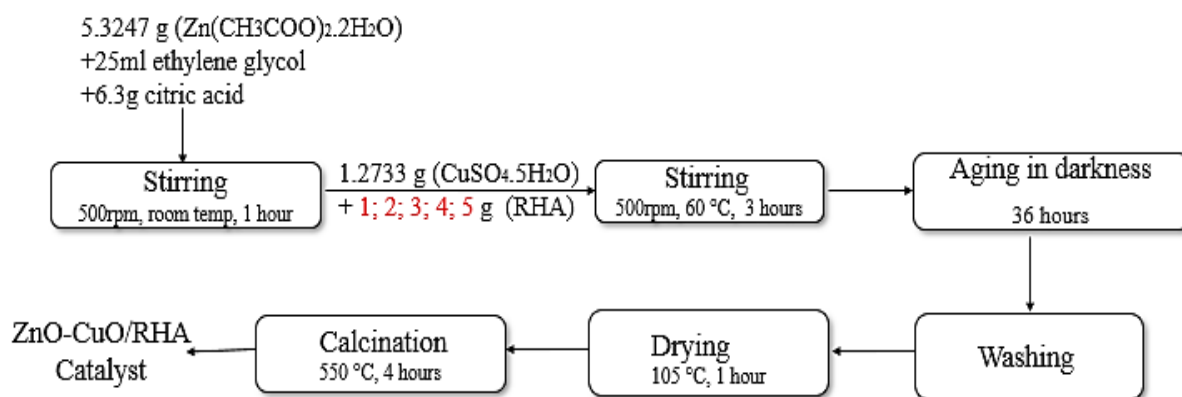


Figure 1: Procedure for Synthesis of ZnO-CuO/RHA [21]

During the experiments 5 ml of the sample was withdrawn from the beaker at a 30 minutes interval and centrifuged at 2500 rpm for 20 minutes to be analysed by a UV-Vis spectrophotometer to obtain final concentration. The same procedure was used for every experiment. The percentage of photocatalytic degradation was calculated using the equation

$$\text{Degradation} = \left(\frac{C_0 - C_t}{C_0} \right) * 100 \quad \text{Eqn. 1}$$

where C_0 = Initial concentration of methylene blue
 C_t = Final concentration of methylene blue after irradiation.

2.2.4 Preliminary screening and Comparative degradation efficiency

The 5 different synthesized ZnO-CuO /RHA catalysts were analyzed under the same conditions of catalyst dosage 0.1 g, in 100 mL of 15ppm MB concentration for 3 hours (180 minutes) and the catalyst that consistently gave the highest percentage of degradation was selected as the choice catalyst for the process. The photocatalytic degradation was conducted using control catalysts (ZnO, CuO, RHA and a blank sample) to perform a comparative analysis with the selected best catalyst.

2.3 Catalyst characterisation

The synthesized catalyst (ZnO-CuO/RHA) was characterized to ascertain some of its properties using Scanning Electron Microscope with energy Dispersive X-ray Spectroscopy (SEM-EDS), Fourier Transform Infra-Red Spectroscopy (FTIR) and Brunauer-Emmet-Teller (BET) analysis. Scanning electron microscope X-ray energy dispersion spectrum (SEM-EDX, Leo 1532 VP, Germany) facilitated the determination of the surface structure or morphology and chemical composition analysis of the catalyst. FTIR was conducted to determine the functional groups of the precursors and synthesized samples with (Shimadzu, FTIR-8400S, Japan) Spectrometer within the range of 400 and 4000 cm⁻¹ of the FTIR spectra. The FTIR technique was used to identify the surface functional groups, which are necessary for either surface or subsurface adsorption that occurs during the photocatalysis. The FTIR spectroscopy serves as an important means of highlighting the nature of the adsorbed species [22]. The surface area, pore diameter, pore volume and size of the catalysts

were studied using the Brunauer-Emmett-Teller (BET) method (SHIMADZU SS-100). The catalyst was characterized by N₂ adsorption test at 77 K. 100 ml/min of dry nitrogen, introduced into the sample tube to prevent contamination of the clean surface, then the sample tube was removed and the sample weighed. The sample tube was fixed to the volumetric apparatus, and then the sample was evacuated to 2 Pa pressure. Adsorbate was introduced to give the lowest desired relative pressure, and then the volume adsorbed was measured.

3. Results and Discussion

3.1 Synthesis

The catalyst prepared varied in weights due to the different weights of RHA present therein. However, they all exhibited similar physical appearance i.e., all synthesized particles were black in colour and smoothly distributed with no agglomeration in the bulk appearance. 25%CuO-ZnO exhibited desired properties and was adopted for our study with rice husk ash as support.

3.2 Preliminary Screening

The photodegradation efficiency of ZnO-CuO/RHA on 15mg/l of methylene blue having varied weights of rice husk ash (RHA) were analyzed. As shown in **Figure 3** The degradation percentage of the ZCR catalyst with 1, 2, 3, 4, and 5 wt. % of RHA were established to be 80.31%, 88.23%, 99.94%, 91.06 % and 81.12% respectively after 180 minutes. Upon increasing the weight of rice husk ash incorporated into the matrix from 4 grams to 5 grams the degradation efficiency decreased to 91.06% and 81.12 %, respectively, this may be attributed to the accumulation of RHA on the surface of ZnO-CuO that causes a reduction in the light being penetrated unto the active sites of the photocatalyst. With higher RHA weight, activated molecules are deactivated due to the collision with the molecules in the ground state which dominates the reaction, thereby slowing down the reaction rate and increasing time required for degradation. The photocatalytic activity against irradiation time given in **Figure 4** shows that the catalysts give a linear relationship with increase in time. Hence, the ZnO-CuO with 3 g of RHA was selected as the best catalyst composition for the photodegradation process.

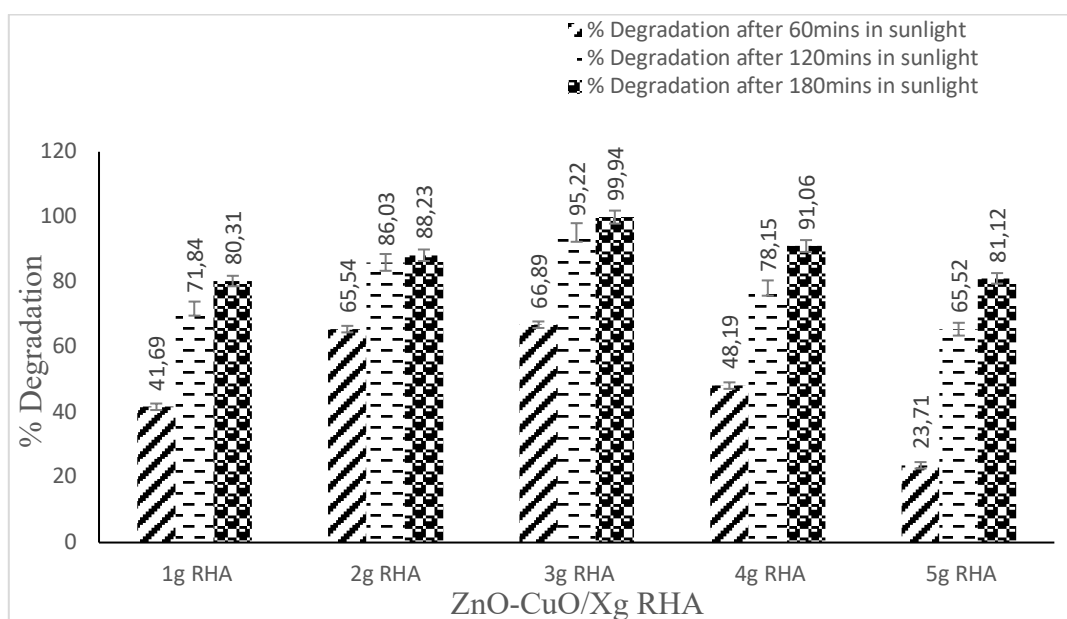


Figure 2: Catalytic activity of different RHA wt. % (ZnO-CuO/RHA) on the photodegradation of MB

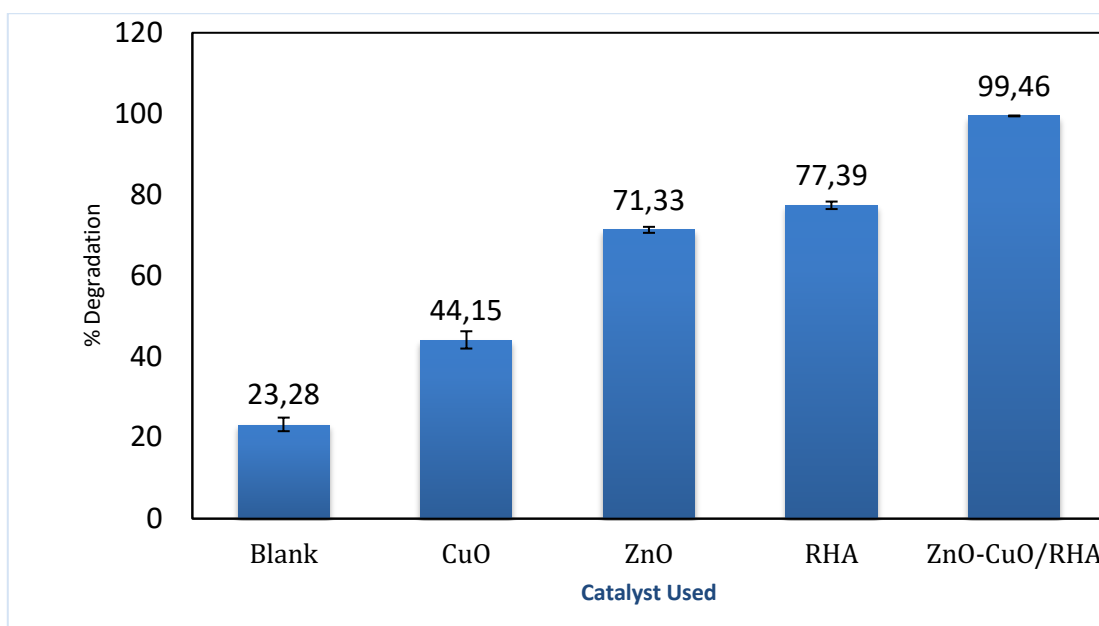


Figure 3: Photocatalytic Activity of MB using Control Catalyst

The degradation of MB with a blank solution (no catalyst), with ZnO, CuO, RHA and the ZnO-CuO/RHA catalyst was conducted using the same conditions as the preliminary screen and the result is shown in **Figure 3**. to be 23.28%, 44.15%, 71.33%, 77.39% and 99.46 % respectively after 3hours. From **Figure 3**, the concentration ratio against time is given and it is observed that there is no remarkable degradation with the blank sample, this is due to the absence of a catalyst. The plot in **Figure 3** shows a notable increase in the photocatalytic activity of the synthesized catalyst, this implies that the catalyst synthesized has higher degradation activity in the degradation of methylene blue when compared with the singular control catalyst. Probable reasons for this is the resultant increase in the surface area of the synthesized catalyst after coupling with rice husk ash an agricultural waste with high surface area [23] which enables the ZnO-CuO/RHA catalyst to have a more active site leading to faster and higher degradation of the dye. According to [24], the reactants that aid degradation of organic dyes includes free radicals like the hydroxyl radicals and super oxide anions generated when hydrogen peroxide (H_2O_2) is broken down. It was observed that the ZnO-CuO/RHA catalysts has higher degradation in the presence of sunlight when compared with zinc oxide, copper (II) oxide and rice husk ash individually, likely due to reduction in bandgap energy levels by tuning the valence bands of ZnO with CuO and the higher surface area of the catalyst.

3.3 Product composition

The composition of the products was determined using Energy Dispersive X-ray spectroscopy (EDS). The spectrums and the summarized results are shown in **Figures 4a-b** The EDX of the rice husk ash showed high content of silicon, followed by magnesium, calcium, iron and presence of other oxides which recorded the weight percent of the significant elements as silicon (60wt.%), oxygen (15.0 wt.%), carbon (5.5 wt.%), the other elemental compositions might be due to pre and post treatment process effect of the rice husk ash. The chemical composition of the ZnO-CuO/RHA composite gave prominent peaks of silicon (Si), copper (Cu), and Zinc (Zn) while observed subsided peaks includes oxygen (O) and carbon (C). This reveals that the obtained ZnO-CuO/RHA composite is evenly distributed with traces of carbon, likely due to calcination and the coating from the SEM.

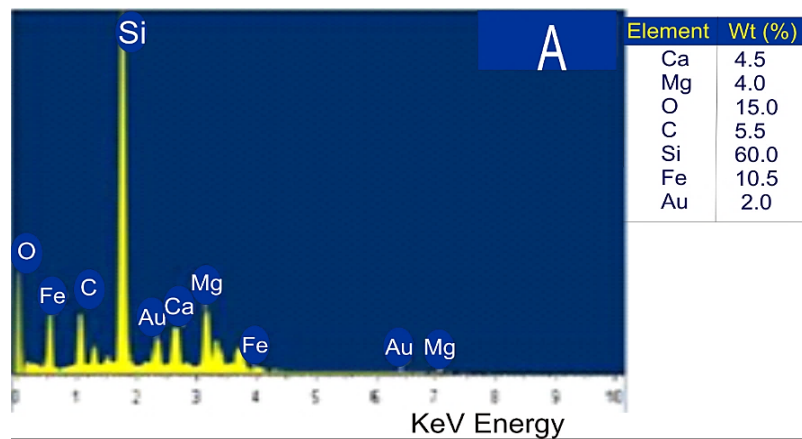


Figure 4a. EDX analysis of Rice Husk Ash

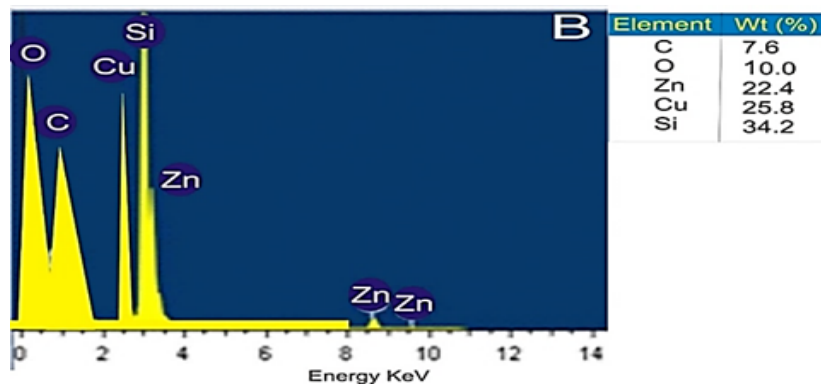


Figure 4b. EDX analysis of ZnO-CuO/RHA Composite

3.4 Surface Morphology

The surface morphology of the products was determined using SEM. Figures 5 and 6 shows the SEM micrographs of the prepared rice husk ash and as-synthesized ZnO-CuO/RHA photocatalyst.

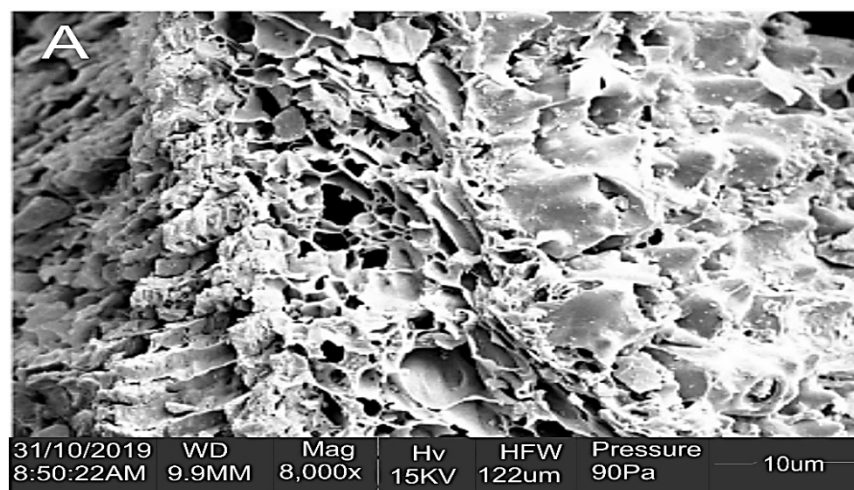


Figure 5. SEM micrograph of Rice Husk Ash, at (a) 8000×

The surface morphology of the rice husk ash as studied using SEM appears to have been heterogeneously processed into a solid irregular hollow structure with tiny voids. The flaky (plate like) morphology of rice husk ash in the image shows the surface is loosely bound thereby making them highly amorphous and reactive [15]. The SEM image show that many residual pores are

distributed within the rice husk ash samples, which depicts surface protrusion with most of the silica embedded in the outer or epidermal cells leaving an active and highly porous material with a large internal surface area as reported by [25].

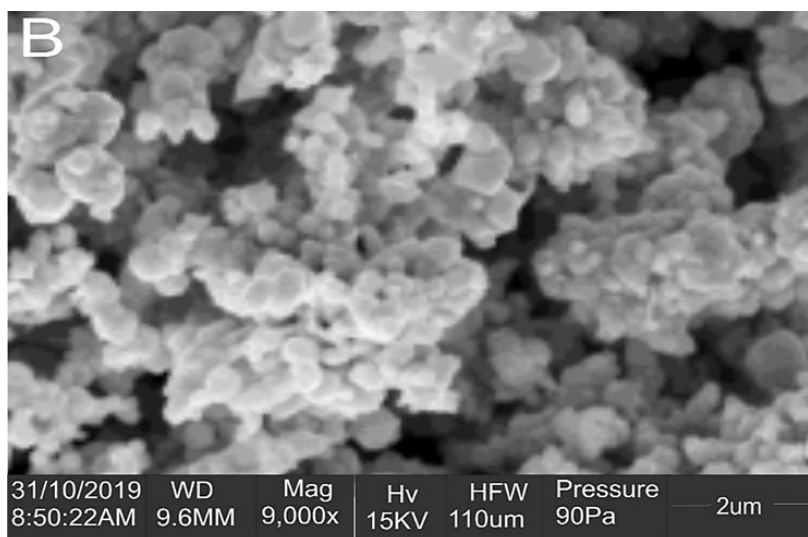


Figure 6a. SEM micrograph of ZnO-CuO/RHA Photocatalyst, at (a) 9000×

The SEM analysis in **Figure 6a** revealed large pores, smooth edges, and agglomeration on the surface of the catalyst. The different constituents appear to have been homogeneously processed into solid particles of varying dimensions and having a flower/ petal shape. Accumulation of varied nanosheet on a solitary point produced this morphology caused by the intrinsic anisotropic growth of ZnO-CuO crystals on the surface of the rice husk ash, the observed particle shapes are spherical in nature [26]. The image shows the uniform distribution of nano spheres on the surface of RHA and the agglomerations is attributed to the amorphous nature of the rice husk ash that is predominately SiO as evidenced from the EDX analysis.

3.4.1 Particle Size Distribution Analysis from SEM image

The particle size was calculated from scanning electron micrograph using the Image J (V8) software. The particle size distribution from the SEM image was analyzed and the plot is given in **Figure 6b**. From the SEM image, each sheet has a size of about 10 μm, with that of the full flower-like structure within the range 3 and 4 μm, (**Figure 6b**) the prepared ZnO-CuO/RHA exhibits average particle size of 3.57916 μm. This value differs from that of [21], which was 15.74 nm. The addition of rice husk ash is the plausible reason for the larger particle sizes obtained in this study.

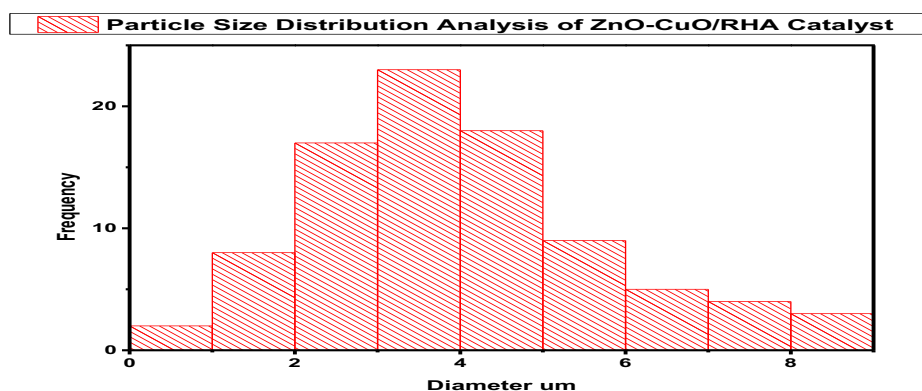


Figure 6b: Particle size distribution of ZnO-CuO/RHA

3.5 Functional groups

FTIR spectra of the precursors and samples synthesized are shown in **Figures 7a and 7b**. The FTIR spectra of the synthesized ZnO-CuO/RHA catalyst and RHA is given in **Figure 7a** and the peaks at 1651 cm^{-1} and 1527 cm^{-1} are due to the symmetric and asymmetric stretching modes of carboxylate ions while the broad band at $2950\text{--}3250\text{ cm}^{-1}$ is due to O–H stretching vibration of the hydroxyl group which is attributed to the adsorbed surface water (attached via Van der Waals bonds) or free hydroxyl group for RHA [23] and silanol group (SiOH) for the ZnO-CuO/RHA [27].

The band responsible for Si-O-Si groups at 1100 cm^{-1} was observed in all the samples due to the presence of Silica which is the major constituent of RHA with the peaks at 1033 to 2950 showing the SiO and CH₂ symmetric and asymmetric stretching at 1527 the Si-O-Si linkage is observed in the crystalline phase. The peaks at 921 cm^{-1} and 462 cm^{-1} is assigned to the C–C stretching mode and M–O stretching vibrations respectively (M = metal). At 832 cm^{-1} and 623 cm^{-1} , the weak bands observed are due to the frequency vibrations caused by changes in the structural features when Cu was added into the Zn–O and Si–O lattices. The Zn–O bond is shown at stretching frequency of 550 cm^{-1} for pure ZnO which shifted to a higher frequency of 754 cm^{-1} .

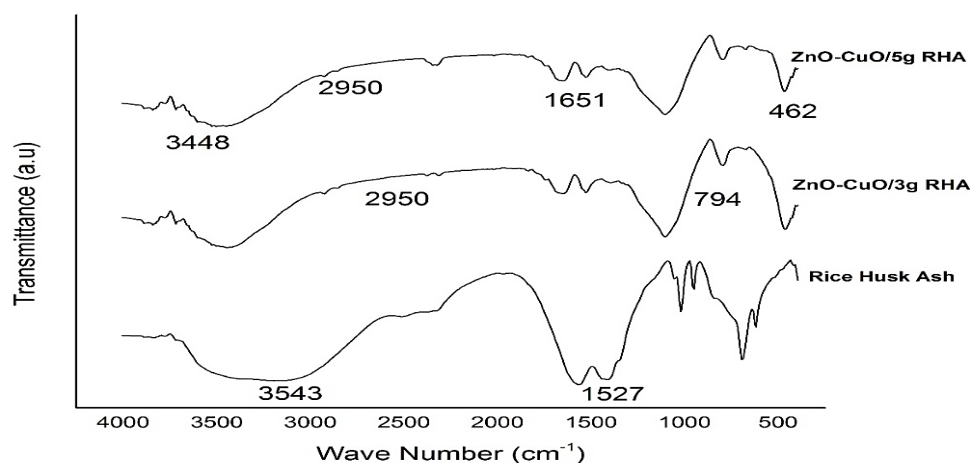


Figure 7a: FTIR Spectra of Synthesized ZnO-CuO/RHA and RHA

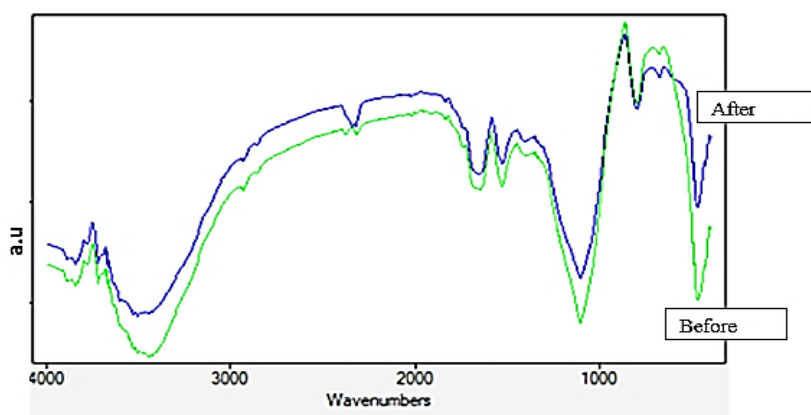


Figure 7b: FTIR Spectra of Optimal ZnO-CuO/RHA before (green) and after (blue) MB photodegradation

Figure 7b shows the FTIR spectra of the selected catalyst before and after the process of photocatalysis. The broad absorption peaks between 3450 cm^{-1} and 1100 cm^{-1} are ascribed to the polymeric O–H stretching vibration in the Zn–Cu–Si–O lattice [28]. The sharp peak at 1645 cm^{-1} is

due to the H–O–H bending vibration, which is assigned to the H₂O in the ZnO. The peaks at 3450, 1100 and 642 cm⁻¹ affirm adsorption of carboxylate ions on the surface of the ZnO-CuO/RHA catalyst. The sharp peak at 1051.1 cm⁻¹ is due to the rich presence of the silica group which depicts the complete removal of impurities and the organic component during the photocatalysis process.

3.6 BET

Single-point Brunauer–Emmett–Teller (BET) analysis was used to calculate the specific surface area and pore parameters of the samples after conducting N₂ adsorption of the samples at 77 K. The data from N₂ adsorption desorption isotherms demonstrated that the ZnO-CuO/RHA photocatalyst is porous with a surface area of 36.0067 ± 2.6426 m²/g, while the pore diameter and pore volume are 8.50nm and 42.153365 cc/g, respectively. The rice husk ash (Table 1) showed surface area of 39.6215 m²g⁻¹ compared to that of ZnO-CuO with 28.965 m²g⁻¹ While the composite showed an encouraging higher BET surface area of 36.0067 ± 2.6426 m²/g. This could be ascribed to the higher surface area of rice husk ash on introduction into the pores of the ZnO-CuO. The high surface area and porosity can promote photocatalysis site availability and adsorption of pollutants through the composite, having the potential to conveniently accommodate MB molecular dimension [29].

Table 1: BET Results for ZnO-CuO, Rice Husk Ash, and ZnO-CuO/RHA

Properties	ZnO-CuO	Rice Husk Ash	ZnO-CuO/RHA
Specific Surface area (m ² /g)	28.9650	39.6215	36.0067
Pore Volume (cc/g)	25.0900	16.1030	42.1534
Pore Diameter (nm)	11.60	19.54	8.50

3.7 Powder X-ray Diffraction Analysis

The crystallographic properties of the samples were examined by powder X-ray diffraction (PXRD) as presented in Figure 8. The pattern of ZnO-CuO/RHA exhibits the existence of zincite (ZnO), tenorite (CuO) and cristobalite, quartz (RHA).

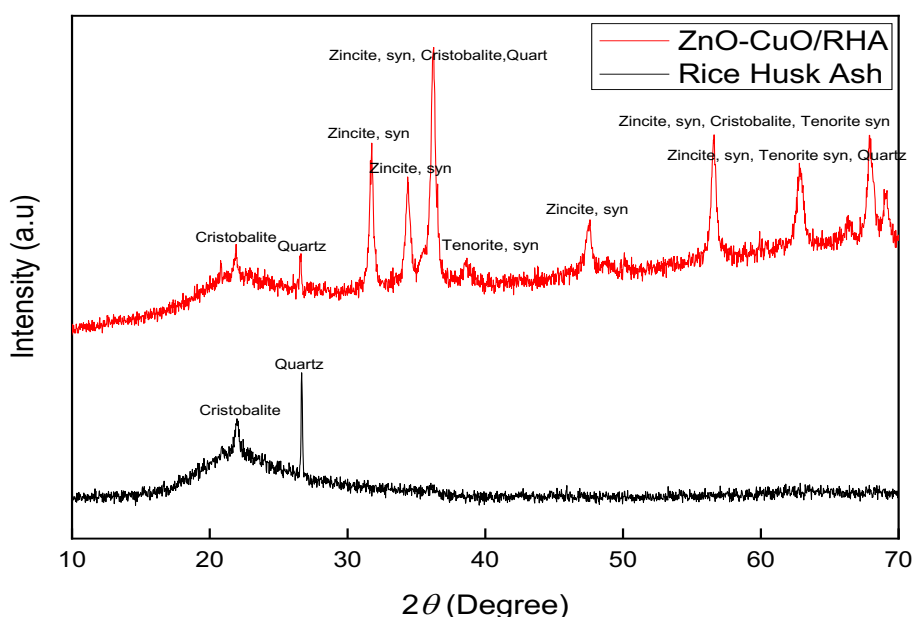


Figure 8: XRD Patterns of ZnO-CuO/RHA Catalyst and RHA

The XRD pattern given in **Figure 8** show the ZnO diffraction lines appeared at peak 2θ of 31.87° , 34.19° , 36.96° , 48.32° and 63.85° . The CuO peak appears at 2θ of 38.03° while the RHA appears at 2θ peaks of 22.34° and 26.87° . These are similar to what [21] obtained (ZnO $2\theta = 67^\circ$; and CuO $2\theta = 38^\circ$). The synthesised ZnO-CuO/RHA has peak 2θ at 36.75° , 57.39° , 66.42° , and 69.73° . The observed peaks are in agreement with the crystal planes in the Joint Committee on Powder Diffraction Standard (JCPDS) card numbers of ZnO, CuO and SiO: JCPDS 36-1451 that has the ZnO peak at $2\theta = 31.7^\circ$; 34.4° ; 36.2° ; 62.8° ; 67.9° ; 69.05° , JCPDS 05-0661 that has the CuO peak at $2\theta = 30^\circ$ to 50° and JCPDS 021-1272 that has SiO (RHA) peak at $2\theta = 22^\circ$ [29]. The XRD results detected no impurity peaks and thus indicated the high purity of the composite.

Conclusion

The study successfully synthesised ZnO-CuO/RHA photocatalyst having a flower-like morphology *via* sol-gel method modified by adding an agro-based RHA as support. SEM-EDX analysis and FTIR spectroscopy confirmed the incorporation of ZnO and CuO on RHA. Larger surface area was observed for the prepared photocatalyst, increasing the active site for efficient use as a photocatalyst in comparison to bare ZnO-CuO. Aside retaining the photocatalytic properties (2θ peaks at 36.75° , 57.39° , 66.42° , and 69.73° for ZnO-CuO/RHA were in concurrence with the crystal planes in the Joint Committee on Powder Diffraction Standard (JCPDS) card numbers JCPDS 36-1451 of ZnO, CuO and SiO), the catalytic material exhibited further improvement such as increased surface area of $36.0067 \text{ m}^2/\text{g}$ against the open literature value of $28.74 \text{ m}^2/\text{g}$. Similarly, the FTIR showed vibrations at 470.65 cm^{-1} , 694.40 cm^{-1} and 2330.09 cm^{-1} for ZnO, CuO and RHA (SiO), respectively. The modified sol-gel method studied serves as a simpler process to produce a low-cost photocatalyst with high stability and surface area, resulting in a material suitable for use in environmental purification after testing for the photocatalytic degradation of methylene blue dye.

Acknowledgement

The technical inputs of Mr Ogwuche of Chemistry Department and all my supervisors are acknowledged.

Disclosure statement: *Conflict of Interest:* The authors declare that there are no conflicts of interest. *Compliance with Ethical Standards:* This article does not contain any studies involving human or animal subjects.

References

- [1] S. Shakoor and A. Nasar, 'Adsorptive treatment of hazardous methylene blue dye from artificially contaminated water using cucumis sativus peel waste as a low-cost adsorbent', *Groundw. Sustain. Dev.*, 5 (2019) 152-159, doi:10.1016/j.gsd.2019.06.005.
- [2] X.Chen, F. Zhang, Q. Wang, X. Han, X. Li, J. Liu, H. and Lin, F. Qu, 'The synthesis of ZnO/SnO₂ porous nanofibers for dye adsorption and degradation', *R. Soc. Chem.*, 44(7) (2015) 3034-3042, doi: 10.1039/c4dt03382e.
- [3] S. Haslinger, Y. Wang, M. Rissanen, M. B., Lossa, M. Tanttu, E. Ilen, M. Määttänen, A. Harlin, M. Hummel and H. Sixta, 'Recycling of vat and reactive dyed textile waste to new colored man-made cellulose fibers', *Green Chem.*, 21(20) (2019) 5598–5610, doi: 10.1039/c9gc02776a.

- [4] M. Hassaan and A. El Nemr, 'Advanced Oxidation Processes (AOPs) for Wastewater Treatment Advanced Oxidation Processes of Some Organic Pollutants in Fresh and Sea Water', *Am. J. Environ. Sci. Eng.*, 1(3) (2017) 64-67, doi: [10.11648/j.ajese.20170103.11](https://doi.org/10.11648/j.ajese.20170103.11).
- [5] L. Shi *et al.*, 'Functional rice husk as reductant and support to prepare as-burnt Cu-ZnO based catalysts applied in low-temperature methanol synthesis', *Catal. Commun.*, 89 (2017) 1–3, doi: [10.1016/j.catcom.2016.10.011](https://doi.org/10.1016/j.catcom.2016.10.011).
- [6] F. Iracà and M. Romero, 'Abstract review on: Current treatment technologies and practical approaches on textile wastewater Dyes Removal', (2017). Available: www.pantareiwater.com. Accessed on Feb 21, 2019
- [7] M. A. H. Devadi, M. Krishna, H. N. N. Murthy, and B. S. Sathyanarayana, 'Statistical Optimization for Photocatalytic Degradation of Methylene Blue by Ag-TiO₂ Nanoparticles', *Procedia Mater. Sci.*, 5 (2016) 612–621, doi: [10.1016/j.mspro.2016.07.307](https://doi.org/10.1016/j.mspro.2016.07.307).
- [8] C. K. N. Peh, M. Gao, and G. W. Ho, 'Harvesting broadband absorption of the solar spectrum for enhanced photocatalytic H₂ generation', *J. Mater. Chem. A*, 3(38) (2015) 19360–19367, doi: [10.1039/c5ta05042a](https://doi.org/10.1039/c5ta05042a).
- [9] Y. T. Prabhu, V. Navakoteswara Rao, M. V. Shankar, B. Sreedhar, and U. Pal, 'The facile hydrothermal synthesis of CuO@ZnO heterojunction nanostructures for enhanced photocatalytic hydrogen evolution', *New J. Chem.*, 43(17) (2019) 6794–6805, doi: [10.1039/c8nj06056h](https://doi.org/10.1039/c8nj06056h).
- [10] Q. Zhou, 'Synthesis of Vertically-Aligned Zinc Oxide Nanowires and Their Applications as Photocatalysts', *MSc. thesis, Mech. Eng.-Nanotech*, University of Waterloo, Ontario, Canada, (2018). Accessed on Feb 15, 2019
- [11] A. L. Subramanian, S. Thirupathi, M. M. Sathath, and M. Kannan, 'Investigation on Thermal Properties of CuO–ZnO Nanocomposites', *Natl. Acad. Sci. Lett.*, 42(1) (2018) 81–85, doi: [10.1007/s40009-018-0723-1](https://doi.org/10.1007/s40009-018-0723-1).
- [12] K. M. Lee, C. W. Lai, K. S. Ngai, and J. C. Juan, 'Recent developments of zinc oxide based photocatalyst in water treatment technology: A review', *Water Research*, Elsevier Ltd, 88 (2017) 428–448, doi: [10.1016/j.watres.2017.09.045](https://doi.org/10.1016/j.watres.2017.09.045).
- [13] E. Peter Etape, L. John Ngolui, J. Foba-Tendo, D. M. Yufanyi, and B. Victorine Namondo, 'Synthesis and Characterization of CuO, TiO₂, and CuO-TiO₂ Mixed Oxide by a Modified Oxalate Route', *J. Appl. Chem.*, 1 (2017) 1–10, doi: [10.1155/2017/4518654](https://doi.org/10.1155/2017/4518654).
- [14] F. W. Chang, W. Y. Kuo, and H. C. Yang, 'Preparation of Cr₂O₃-promoted copper catalysts on rice husk ash by incipient wetness impregnation', *Appl. Catal. A Gen.*, 288(2) (2015) 53–61, doi: [10.1016/j.apcata.2015.04.046](https://doi.org/10.1016/j.apcata.2015.04.046).
- [15] A. Ikhlaiq, S. Azhar, M. A. Kazmi, N. Ramzan, and M. Rustam, 'Methylene Blue removal from Aqueous Solutions by using Rice Husk Ash (RHA) and Peanut Shell Ash (PSA)', *J. Fac. Eng. Technol.*, 21(3) (2018) 1- 8.
- [16] Y. C. Zhang, Z. N. Du, K. W. Li, M. Zhang, and D. D. Dionysiou, 'High-performance visible-light-driven SnS₂/SnO₂ nanocomposite photocatalyst prepared via in situ hydrothermal oxidation of SnS₂ nanoparticles', *ACS Appl. Mater. Interfaces*, 3(5) (2020) 1528-1537, doi: [10.1021/am200102y](https://doi.org/10.1021/am200102y).
- [17] R. K. Sharma and R. Ghose, 'Synthesis of nanocrystalline CuO-ZnO mixed metal oxide powder by a homogeneous precipitation method', *Ceram. Int.*, 40(7) (2016) 10919–10926, doi: [10.1016/j.ceramint.2016.03.089](https://doi.org/10.1016/j.ceramint.2016.03.089).

- [18] J. Xie, Z. Zhou, Y. Lian, Y. Hao, P. Li, and Y. Wei, 'Synthesis of α -Fe₂O₃/ZnO composites for photocatalytic degradation of pentachlorophenol under UV-vis light irradiation', *Ceram. Int.*, 41(2) (2018) 2622–2625, doi: [10.1016/j.ceramint.2018.10.043](https://doi.org/10.1016/j.ceramint.2018.10.043).
- [19] S. Das and V. C. Srivastava, 'An overview of the synthesis of CuO-ZnO nanocomposite for environmental and other applications', *Nanotechnology Reviews*, Walter de Gruyter GmbH, 7(3) (2018) 267–282, doi: [10.1515/ntrev-2018-0144](https://doi.org/10.1515/ntrev-2018-0144).
- [20] N. Widiarti, J. K. Sae, and S. Wahyuni, 'Synthesis CuO-ZnO nanocomposite and its application as an antibacterial agent', in *IOP Conference Series: Materials Science and Engineering*, 172(1) (2017) 20-36, doi: [10.1088/1757-899X/172/1/012036](https://doi.org/10.1088/1757-899X/172/1/012036).
- [21] P. V. Adhyapak, S. P. Meshram, V. Tomar, D. P. Amalnerkar, and I. S. Mulla, 'Effect of preparation parameters on the morphologically induced photocatalytic activities of hierarchical zinc oxide nanostructures', *Ceram. Int.*, 39(7) (2018) 7367-7378, doi: [10.1016/j.ceramint.2018.02.076](https://doi.org/10.1016/j.ceramint.2018.02.076).
- [22] Y. Y. Shu-Ting Liu, Xue-Gang Chen, Ao-Bo Zhang, Kang-Kang Yan, 'Electromagnetic Performance of Rice Husk Ash', *BioResources*, 9(2) (2019) 2328–2340, doi: [10.15376/biores.9.2.2328-2340](https://doi.org/10.15376/biores.9.2.2328-2340).
- [23] S. Zaman, A. Zainelabdin, G. Amin, O. Nur, and M. Willander, 'Efficient catalytic effect of CuO nanostructures on the degradation of organic dyes', *J. Phys. Chem. Solids*, 73(11) (2018) 1320–1325, doi: [10.1016/j.jpics.2018.07.005](https://doi.org/10.1016/j.jpics.2018.07.005).
- [24] A. A. Abiodun, Y. O. Jimoh, 'Microstructural Characterisation, Physical and Chemical Properties of Rice Husk Ash as Viable Pozzolan In Building Material: A Case Study of Some Nigerian Grown Rice Varieties', *Niger. J. Technol.*, 37(1) (2018) 71-77, doi: <http://dx.doi.org/10.4314/njt.v37i1.10>.
- [25] J. M. S. Tenzin Tenkyong, Neena Bachan, J. Raja, P. Naveen Kumar, 'Investigation of sol-gel processed CuO / SiO₂ nanocomposite as a potential photoanode material', *Mater. Sci. Pol.*, 33(4) (2017) 826-834, doi: [10.1515/msp-2017-0097](https://doi.org/10.1515/msp-2017-0097).
- [26] B. Allabergenov, U. Shaislamov, H. Shim, M.-J. Lee, A. Matnazarov, and B. Choi, 'Effective control over near band-edge emission in ZnO/CuO multilayered films', *Opt. Mater. Express*, 7(2) (2017) 494- 501, doi: [10.1364/ome.7.000494](https://doi.org/10.1364/ome.7.000494).
- [27] A. Shokri and M. M. Ghazi, 'Preparation and characterizations of CuO doped ZnO nanostructure for the photocatalytic degradation of 4-chlorophenol under visible light', *Adv. Environ. Technol.*, 1 (2016) 11-24, doi: [10.22104/aet.2016.325](https://doi.org/10.22104/aet.2016.325).
- [28] R. M. Mohamed, M. A. Al-Rayyani, E. S. Baeissa, and I. A. Mkhaldid, 'Nano-sized Fe-metal catalyst on ZnO–SiO₂: (photo-assisted deposition and impregnation) Synthesis routes and nanostructure characterization', *J. Alloys Compd.*, 509(24) (2017) 6824–6828, doi: [10.1016/j.jallcom.2017.03.098](https://doi.org/10.1016/j.jallcom.2017.03.098).
- [29] A. A. A.-A. Hind A. Jassim, Abdulhadi Khadhim, 'Photo Catalytic Degradation of Methylene Blue by Using CuO Nanoparticles', *Int. J. Comput. Appl. Sci. IJOCAAS*, 1(3) (2016) 1-5.

(2021) ; <http://www.jmaterenvirosci.com>